7-2014

Path Loss Modeling for V2V Communication on a Slope

Pengyu Liu

David W. Matolak
University of South Carolina - Columbia, matolak@cec.sc.edu

Bo Ai

Ruoyu Sun

Publication Info

Postprint version. Published in *IEEE Transactions on Vehicular Technology*, Volume 63, Issue 6, 2014, pages 2954-2958.

VI. Conclusion

We have discussed multiuser multicell detection through BSC in an uplink high-frequency reuse scenario. DID has been introduced as an interference mitigation technique for networked MIMO systems. We have compared soft and hard information exchange and cancelation schemes and proposed a novel hard information exchange strategy based on the concept of RMP. The proposed DID-RMP algorithm significantly reduces the backhaul data compared with the soft information exchange while it obtains a better BER performance.

References

[1] D. Gesbert, S. Hanly, H. Huang, S. Shamai Shitz, O. Simeone, and Y. Wei, "MultiD-Cell MIMO cooperative networks: A new look at interference," *IEEE J. Sel. Areas Commun.*, vol. 28, no. 9, pp. 1380–1408, Dec. 2010.

[2] P. Marsch and G. Fettweis, "Uplink CoMP under a constrained backhaul and imperfect channel knowledge," *IEEE Trans. Wireless Commun.*, vol. 10, no. 6, pp. 1730–1742, Jun. 2011.

[3] H. Dai, A. F. Molisch, and H. V. Poor, "Downlink capacity of interference-limited MIMO systems with joint detection," *IEEE Trans. Wireless Commun.*, vol. 3, no. 2, pp. 442–453, Mar. 2004.

[4] T. Mayer, H. Jenkac, and J. Hagenauer, "Turbo base-station cooperation for intercell interference cancellation," in *Proc. IEEE Int. Conf. Commun.*, Jun. 2006, vol. 11, pp. 4977–4982.

[5] S. Khattak, W. Rave, and G. Fettweis, "Distributed iterative multiuser detection through base station cooperation," *EURASIP J. Wireless Commun. Netw.*, vol. 2008, no. 17, pp. 1–15, Jan. 2008.

[6] P. Li, R. C. de Lamare, and R. Fa, "Multiple feedback successive interference cancellation detection for multiuser MIMO systems," *IEEE Trans. Wireless Commun.*, vol. 10, no. 8, pp. 2434–2439, Aug. 2011.

[7] P. Li and R. C. de Lamare, "Parallel multiple candidate interference cancellation with distributed iterative multi-cell detection and base station cooperation," in *Proc. 2012 Int. ITG WSA*, Mar. 7–8, 2012, pp. 92–96.

[8] W. Choi, J. G. Andrews, and C. Yi, "The capacity of multicellular distributed antenna networks," in *Proc. Int. Conf. Wireless Netw., Commun. Mobile Comput.*, Jun. 2005, pp. 1337–1342.

[9] W. Choi and J. G. Andrews, "Downlink performance and capacity of distributed antenna systems in a multicell environment," *IEEE Trans. Wireless Commun.*, vol. 6, no. 1, pp. 69–73, Jan. 2007.

[10] X. Wang and H. V. Poor, "Iterative (Turbo) soft interference cancellation and decoding for coded CDMA," *IEEE Trans. Commun.*, vol. 47, no. 7, pp. 1046–1061, Jul. 1999.

[11] S. Venkatesan, "Coordinating base stations for greater uplink spectral efficiency in a cellular network," in *Proc. IEEE 18th Int. Symp. Pers., Indoor Mobile Radio Commun.*, Athens, Greece, Sep. 2007, pp. 1–5.

[12] S. Khattak and G. Fettweis, "Distributed iterative detection in an interference limited cellular network," in *Proc. IEEE 65th Veh. Technol. Conf. Spring*, Apr. 22–25, 2007, pp. 2349–2353.

[13] B. Hochwald and S. T. Brink, "Achieving near-capacity on a multiple-antenna channel," *IEEE Trans. Commun.*, vol. 51, no. 3, pp. 389–399, Mar. 2003.

[14] P. Li and R. C. de Lamare, "Adaptive decision feedback detection with constellation constraints for MIMO systems," *IEEE Trans. Veh. Technol.*, vol. 61, no. 2, pp. 853–859, Feb. 2012.

[15] R. C. de Lamare and R. Sampaio-Neto, "Minimum mean squared error iterative successive parallel arbitrated decision feedback detectors for DS-CDMA Systems," *IEEE Trans. Commun.*, vol. 56, no. 5, pp. 778–789, May 2008.

[16] R. C. de Lamare, R. Sampaio-Neto, and A. Hjorungnes, "Joint iterative interference cancellation and parameter estimation for CDMA systems," *IEEE Commun. Lett.*, vol. 11, no. 12, pp. 916–918, Dec. 2007.

[17] J. W. Choi, A. C. Singer, J. Lee, and N. I. Cho, "Improved linear soft-input soft-output detection via soft feedback successive interference cancellation," *IEEE Trans. Commun.*, vol. 58, no. 3, pp. 986–996, Mar. 2010.

[18] Y. Hadisusanto, L. Thiele, and V. Jungnickel, "Distributed base station cooperation via block-diagonalization and dual-decomposition," in *Proc. IEEE GLOBECOM*, Nov. 30–Dec. 4, 2008, pp. 1–5.

[19] S. Benedetto1, G. Montorsi, D. Divsalar, and F. Pollara, "Soft-input soft-output modules for the construction and distributed iterative decoding of code networks," *Eur. Trans. Telecommun.*, vol. 9, no. 2, pp. 155–172, Mar./Apr. 1998.

Path Loss Modeling for Vehicle-to-Vehicle Communication on a Slope

Pengyu Liu, *Student Member, IEEE*,
David W. Matolak, *Senior Member, IEEE*,
Bo Ai, *Senior Member, IEEE*, and
Ruoyu Sun, *Student Member, IEEE*

***Abstract*—Path loss modeling for both regular and irregular terrains is still gaining significant attention from researchers. A sloped terrain is one specific kind of an irregular terrain that—as far as we are aware—has not been completely studied. Although some results have been published for slope path loss modeling in cellular communication, an adequate model for the case when the transmitter (Tx) and the receiver (Rx) both have low-height antennas and are located on or near a slope does not exist. In this paper, for complete analysis of such conditions, we consider four scenarios: 1) two vehicles are located at opposite ends of the slope; 2) one vehicle is on the slope, and the other vehicle is beyond the slope crest; 3) one vehicle is on the slope, and the other is away from the slope at the bottom; 4) both vehicles are on the slope. For scenarios 1 and 2, we have developed analytical path loss models. We have also made some corroborating measurements for scenario 1. Scenarios 3 and 4 are addressed by models already in the literature. Simulation results for two vehicles traveling toward, on, and then beyond a slope (a sequence of our scenarios) are also shown to illustrate how sloped-terrain path loss varies in contrast to the typical flat-earth condition. Our models for scenarios 1 and 2 add to the literature and can be used to numerically estimate path losses for vehicle-to-vehicle (V2V) communication over a slope.**

***Index Terms*—Path loss, vehicle-to-vehicle (V2V).**

I. Introduction

THE TOPIC of path loss modeling has gained a great deal of attention, for multiple environments, frequency bands, and applications. Despite the rich literature, we have found only limited work on specific models for path loss when the transmitter (Tx) and the receiver (Rx) are both near or on a slope when antennas are at low heights. We provide new results here for cases not specifically addressed in the literature, which are applicable, for example, for vehicle-to-vehicle (V2V) communication systems.

Path loss over irregular terrains has been investigated by a number of researchers over the years. Okumura *et al.* proposed correction factors to the propagation loss curves for sloped-terrain scenarios for

Manuscript received April 15, 2013; revised August 19, 2013, October 5, 2013, and November 16, 2013; accepted November 22, 2013. Date of publication December 11, 2013; date of current version July 10, 2014. This work was supported in part by the National Natural Science Foundation of China under Grant 61222105, by the Fundamental Research Funds for the Central Universities under Grant 2010JBZ008, by the Beijing Municipal Natural Science Foundation under Grant 4112048, by the project of the State Key Laboratory under Grant RCS2012ZT013, by the Key Project for Railway Ministry of China under Grant 2012X008-A, by the interdiscipline cooperation projects of the New Star of Science and Technology supported by Beijing Metropolis under Grant xxhz201201, and by the Key Grant Project of the Chinese Ministry of Education under Grant 313006. The review of this paper was coordinated by Prof. C.-X. Wang. *(Corresponding author: B. Ai.)*

P. Liu and B. Ai are with the State Key Laboratory of Rail Traffic Control and Safety, Beijing Jiaotong University, Beijing 100044, China (e-mail: aibo@ieee.org).

D. W. Matolak and R. Sun are with the Department of Electrical Engineering, University of South Carolina, Columbia, SC 29208 USA (e-mail: matolak@cec.sc.edu; Sun55@email.sc.edu).

Color versions of one or more of the figures in this paper are available online at http://ieeexplore.ieee.org.

Digital Object Identifier 10.1109/TVT.2013.2294721

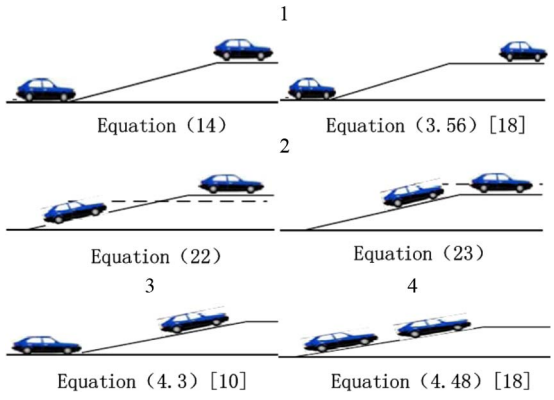

Fig. 1. Four scenarios of communication over a slope.

frequencies 450–900 MHz and path distances 5–10 km [1]. Edwards and Durkin in [2] and Dadson in [3] proposed a terrain-based technique to reconstruct the path loss profile for a point-to-point link between a Tx and an Rx. Longley and Rice [4] introduced methods and a computer program for computing median path loss over an irregular terrain. In [5] and [6], the authors showed that using a single terrain irregularity is not sufficient to represent measured terrain effects with accuracy. Murphy [7] produced a statistical model for predicting propagation loss over an irregular terrain using data collected from several areas. In [8], Lee provided two placement situations for a base station and an Rx communicating over a sloped terrain, for which path loss models were generated. Ohira *et al.* [9] and Nisirat [10] proposed path loss prediction models for a sloped terrain in small-sized cells. All these cited references employ elevated base-station antennas. Wang *et al.* [11] described and classified some important V2V channel measurement campaigns and models. In [12], Cheng *et al.* proposed a dual-slope path loss model (for a flat terrain) for the V2Vchannel at 5.9 GHz in suburban areas, and Karedal *et al.* [13] proposed novel V2V path loss models for urban, suburban, rural, and highway scenarios but did not address the sloped-terrain case. Cheng *et al.* [14] proposed a generic and adaptive geometry-based stochastic model for nonisotropic multiple-input–multiple-output mobile-to-mobile Ricean fading channels but also did not address the sloped-terrain case.

The models by Okumura *et al.* [1], Lee [8], and Ohira *et al.* [9] all concentrated on modeling the path loss over a sloping terrain in cellular communication with an elevated base-station antenna. However, for V2V communication, both Tx and Rx antennas are at low heights ($\sim$1.5 m), significantly differing from the cellular case. Such a feature requires that we consider blockage resulting from the slope edge in some conditions. Furthermore, cellular base stations are usually built at the top or bottom edge of a slope; however, in V2V communication, the vehicles can be anywhere above, below, or on the actual slope, requiring a more careful analysis to accurately model this V2V propagation condition.

There are four scenarios for communication over a slope, as shown in Fig. 1: 1) vehicles are located at opposite ends of the slope, actually off the slope itself; 2) one vehicle is on the slope, whereas the other vehicle is away from the top end, off the slope (or beyond the slope crest); 3) one vehicle is off the slope away from the bottom end, and the other vehicle is on the slope; and 4) both vehicles are on the slope.

In this paper, we derive path loss models for scenarios 1 and 2. The path loss models for scenarios 3 and 4 are addressed by appropriate parameter choices in the "Lee 3-ray model" [8] and the "flat 2-ray model" [15], respectively. We also derive results for the case when one platform (Tx or Rx) or both are at a distance such that the slope's crest blocks either the line of sight (LOS) or ground-reflected component

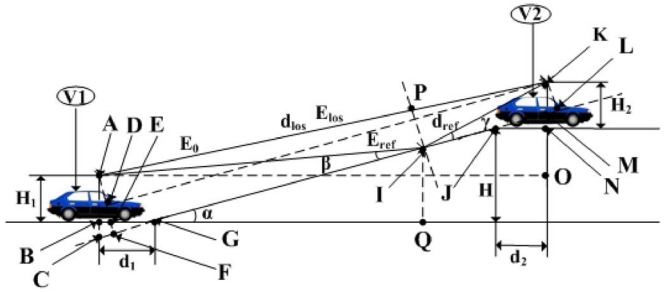

Fig. 2. V2V communication occurring on a slope (scenario 1).

or both in scenarios 1 and 2. Our measurements indicate that the knife-edge diffraction can model the "slope diffraction" of scenario 1 fairly well.

The remainder of this paper is organized as follows. In Section II, we provide the analysis for the slope path loss model for scenarios 1 and 2. Section III presents measurement data that are compared with the theoretical derivation. Section IV contains conclusions.

II. Slope Path Loss Analysis

A. Scenario 1

Here, we have vehicle one $(V1)$ located near the foot of a slope with effective height H and tilt angle α, and vehicle two $(V2)$ is on the top of this slope. This is shown in Fig. 2.

The heights of antennas mounted on vehicles $V1$ and $V2$ are denoted H_1 and H_2, respectively. The distances of the two vehicles from the slope edges are d_1 and d_2, respectively. Simply, geometry gives the LOS distance between the two antennas, i.e., d_{LOS}, as

$$d_{\mathrm{LOS}} = \sqrt{(d_1 + H\cot(\alpha) + d_2)^2 + (H + H_2 - H_1)^2}. \quad (1)$$

Referring to Fig. 1, basic trigonometry yields the following relationships for several of the sides of triangles denoted ΔBCG, ΔJNM, ΔKNL, and ΔADK:

$$AF = (AB + BC)\cos(\alpha) = H_1\cos(\alpha) + d_1\sin(\alpha) \quad (2)$$

$$KL = (KN - MN)\cos(\alpha) = |H_2\cos(\alpha) - d_2\sin(\alpha)| \quad (3)$$

$$AD = AF - FD = H_1\cos(\alpha) + d_1\cos(\alpha) - |H_2\cos(\alpha) - d_2\sin(\alpha)| \quad (4)$$

$$FL = \sqrt{AK^2 - AD^2} = \sqrt{R - S} \quad (5)$$

where we have used $R = (d_1 + H\cot(\alpha) + d_2)^2 + (H_2 + H - H_1)^2$ and $S = (H_1\cos(\alpha) + d_1\cos(\alpha) - |H_2\cos(\alpha) - d_2\sin(\alpha)|)^2$. Using $\Delta\ AFI \sim \Delta\ KLI$, we obtain $AI/KI = AF/KL = FI/(FL - FI)$. Hence

$$FI = AF \cdot FL/(AF + KL) \quad (6)$$

$$AI = \sqrt{AF^2 + FI^2}. \quad (7)$$

Using the obvious relationship $d_{\mathrm{REF}} = AI + IK$ together with (2)–(7), the length of the reflected path is

$$d_{\mathrm{REF}} = \sqrt{R + T} \quad (8)$$

where we have also used $T = 4(H_1\cos(\alpha) + d_1\sin(\alpha))(|H_2\cos(\alpha) - d_2\sin(\alpha)|)$. The length difference between

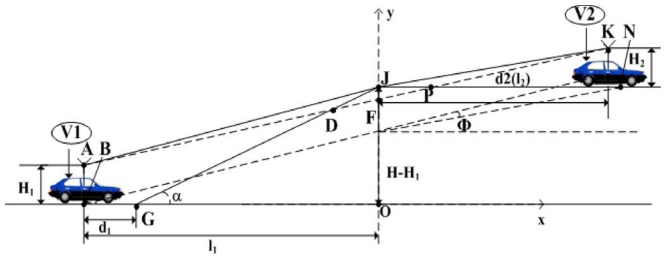

Fig. 3. Slope diffraction model for V2V communication (scenario 1).

the LOS and reflected components is $\triangle d = d_{\mathrm{REF}} - d_{\mathrm{LOS}}$, given by the difference of (1) and (8). The corresponding phase difference is $\triangle\varphi = 2\pi\triangle d/\lambda$.

The field strength at the receiving antenna due to the direct wave is $E_d = E_0/d_{\mathrm{LOS}}$, and the total received field E_i is the sum of the direct and reflected components in scenario 1. (We tacitly assume that the antenna gains for both components are the same.) With the usual assumption that the free-space attenuation of both the direct and reflected components due to distance is essentially the same, we have the total field magnitude as

$$E_i = E_{\mathrm{LOS}} + E_{\mathrm{REF}} = E_d\sqrt{(\cos(\Delta\,\varphi) + \mathbf{\Gamma})^2 + \sin^2(\Delta\,\varphi)} \quad (9)$$

where $\mathbf{\Gamma} = |\Gamma|e^{j\theta}$ is the reflection coefficient of the slope. In this paper, we consider coefficients for both vertical and horizontal polarizations [10] using $\mathbf{\Gamma}_v$ and $\mathbf{\Gamma}_h$ to represent these two reflection coefficients. From [8], the value of the far-field electric fields at the Rx can be written as

$$E_i = (E_0/d_{\mathrm{LOS}})\sqrt{\left(1 + \mathbf{\Gamma}_{v(h)}\right)^2 - 4\mathbf{\Gamma}_{v(h)}\sin^2\left(\frac{\pi}{\lambda}\,\Delta\,d\right)} \quad (10)$$

where E_0 is the transmit field strength at the Tx.

Using (8), (10), and [9, eq. (3.15)] and the geometric parameters d_1, d_2, H, H_1, H_2, and α to compute for R and T, along with wavelength λ and reflection coefficient $\mathbf{\Gamma}_{v(h)}$ to created path loss L_i, we obtain

$$L_i = \frac{16\pi^2 R}{G_t G_r \lambda^2\left|\left(1 + \mathbf{\Gamma}_{v(h)}\right)^2 - 4\mathbf{\Gamma}_{v(h)}\sin^2\left(\frac{\pi}{\lambda}(\sqrt{R+T} - \sqrt{R})\right)\right|}. \quad (11)$$

If one or both of the two vehicles on opposite ends of the sloped terrain are at sufficient distance from the slope's crest (point J in Fig. 2), the LOS path may be obstructed by the slope, and only a diffracted wave can reach the Rx. This situation can be approximated by the knife-edge diffraction model [9]. First, we deduce a critical condition of occurrence of this slope diffraction model.

A coordinate system is set up with origin at point O (0, 0). As shown in Fig. 3, if intersection point F, at coordinates between the direct line between antennas at points A and K and the y-axis, is below point J, the LOS path is entirely blocked. Therefore, when line AK intersects the y-axis at point F, we obtain the critical condition of occurrence of this slope diffraction model. The coordinates of these points are as follows: $F(0, H + H_2 - (H_2 + H - H_1)d_2/[d_1 + d_2 + H\cot(a)])$; $A(-d_1 - H\cot(\alpha), H_1)$; $K(d_2, H_2 + H)$; $J(0, H)$. The straight-line equation for line AK is then easily found as

$$y = [(H_2 + H - H_1)/(d_1 + d_2 + H\cot(\alpha))]\,x + H + H_2 - (H_2 + H - H_1)d_2/(d_1 + d_2 + H\cot(\alpha)). \quad (12)$$

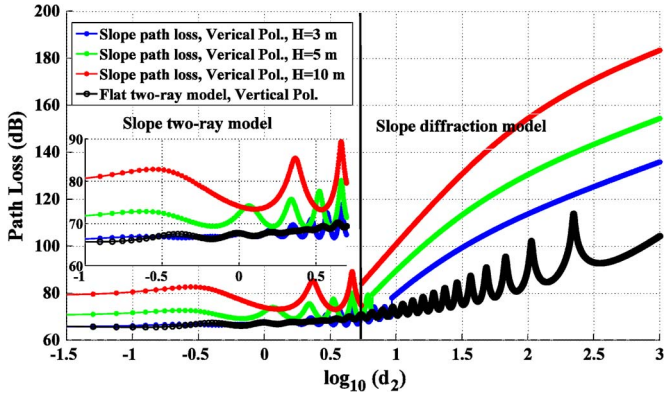

Fig. 4. Path loss of flat 2-ray model and slope path loss model with $H =$ 3 m, 5 m, and 10 m, and $\alpha = \pi/10$ (scenario 1).

Inserting point $J(0, H)$ for the y-value into this line equation, the critical condition can be expressed as

$$H_1 d_2 + H_2 H\cot(\alpha) - H d_2 + H_2 d_1 = 0 \quad (13)$$

and this critical condition can be applied to judge whether a LOS path exists by making (14) above 0 (LOS) or below 0 (non-LOS).

We choose the knife-edge model for the slope diffraction case because of its simplicity. As will be shown later, this is supported by our measurements. Referring to Fig. 2, we can express several additional parameters mathematically. Angle α, distance l_1 from $V1$ to the bottom end of the slope, and distance l_2 from $V2$ to the top end of the slope can be expressed as

$$\Phi = \arctan\left((H - H_1)/(H\cot(\alpha) + d_1)\right) - \arctan(H_2/d_2) \quad (14)$$

$$l_1 = d_1 + H\cot(\alpha) \quad (15)$$

$$l_2 = d_2. \quad (16)$$

Inserting (14)–(16) into [15, eq. (3.56)], the diffraction parameter v is obtained, and then, we apply this to [15, eq. (3.6.1a)–(3.6.1e)] to calculate the extra knife-edge diffraction loss L_d. The path loss between $V1$ and $V2$ is then computed by using the free-space path loss plus diffraction loss L_d.

Example results for this case are shown in Fig. 4. The geometric parameters are slope height $H = 3$ m, 5 m, and 10 m; slope tilt angle $\alpha/10$; distance of $V1$ from the slope end $d_1 = 0$ m; and reflection coefficient $\mathbf{\Gamma}_v$ is computed for vertical polarization for the given incident angle (considering average ground conditions [8]) at 5.2 GHz. In addition, plotted in Fig. 4 for comparison are the flat 2-ray model results. As shown in Fig. 4, the slope path loss model has a fluctuating amplitude for short distances ($-1 \le \log(d_2) \le 1$) and exhibits greater attenuation than the flat 2-ray model by more than 10 dB when the slope height is large. The slope pass loss attenuation then sharply increases when the LOS path is obstructed due to the slope crest, and propagation is only by diffraction. Note that the larger the height of the slope, the shorter the distance at which obstruction occurs, and this effect is analogous to that of increasing the slope tilt angle. When $H = 0$, $\alpha = 0$, and $\mathbf{\Gamma}_v = -1$, our slope 2-ray model will degenerate to the flat 2-ray model [15].

B. Scenario 2

For the scenario of two vehicles, where vehicle $V1$ is on the actual slope with effective height H and tilt angle α, and vehicle $V2$ is on the flat terrain beyond the slope crest, two path loss models are derived for different conditions at small distances; these two conditions are

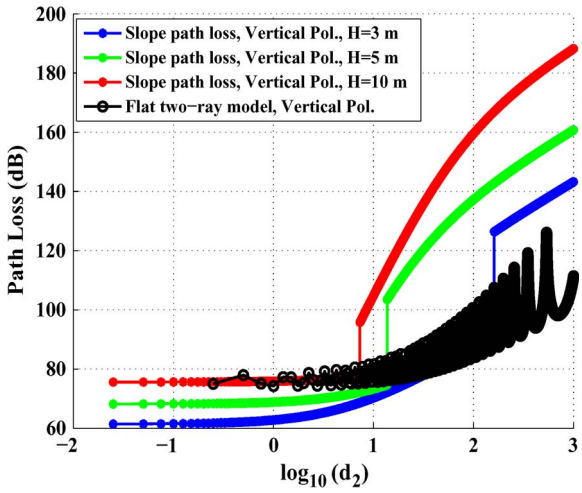

Fig. 5. Path loss of flat 2-ray model and slope path loss with $H =$ 3 m, 5 m, and 10 m, and $\alpha = \pi/10$ (scenario 2).

specified by whether the antenna phase center of vehicle $V1$ is above the slope crest. Because of the similarity to the derivation for scenario 1, for brevity, we only list the primary new equations for this scenario.

When the antenna phase center of $V1$ is below the slope crest, only a LOS path is received at $V2$. In this case, we use a free-space model to express the path loss $L_{ii,1}$ for condition 1, i.e.,

$$L_{ii,1} = -10\log_{10}\left(\frac{G_t G_r \lambda^2}{16\pi^2 U}\right) \tag{17}$$

where we have used $U = (d_1 + H\cot(\alpha) + d_2)^2 + (-H_1' + H + H_2)^2$, and H_1' is the equivalent height of V_1 on the slope, given by $H_1' = |d_1|\tan(\alpha) + H_1/\cos(\alpha)$.

In contrast to the given condition, for the second condition, a LOS component and a component from the flat (top surface) reflection are received at $V2$. The 2-ray path loss $L_{ii,2}$ for condition 2 is

$$L_{ii,2} = -10\log_{10}\left(\frac{G_t G_r \lambda^2}{16\pi^2 U}\right) - 20\log_{10}\left[\left|1 - \exp\left(j\left(\frac{\pi}{\lambda}(\sqrt{V} - \sqrt{W})\right)\right)\right|\right] \tag{18}$$

where $V = (d_1 + H\cot(\alpha) + d_2)^2 + (H_1' - H + H_2)^2$, and $W = (d_1 + H\cot(\alpha) + d_2)^2 + (-H_1' + H + H_2)^2$.

In Fig. 5, three curves are shown to illustrate the variations of the slope path loss in scenario 2 with different slope heights ($H =$ 3 m, 5 m, and 10 m). For small values of d_2, there are fewer path loss fluctuations in scenario 2 than in scenario 1 (cf., Fig. 4); this is because when vehicle $V1$ is on the slope, the slope reflection component is more easily blocked by the slope crest. For the slope diffraction at larger values of d_2, the effect of the diffraction is identical to that of scenario 1.

C. Slope Path Loss Versus Time

A simulation result for communication over a slope for a combination of four scenarios in sequence is described in this section. The simulations all begin with $V1$ (back) and $V2$ (front) at the bottom end of the slope at some initial separation distance from each other. We use $d_{\text{separation}} = 3$ m, 50 m, 100 m, and 500 m. This separation distance remains constant, and in the simulation, the vehicles move with identical constant velocities of 5 m/s toward the slope (height of 3 m and tilt angle of $\pi/10$), onto the slope, then beyond the slope over the simulation duration. The simulation time is 100 s and the spatial sampling interval of the four scenarios is 5 m.

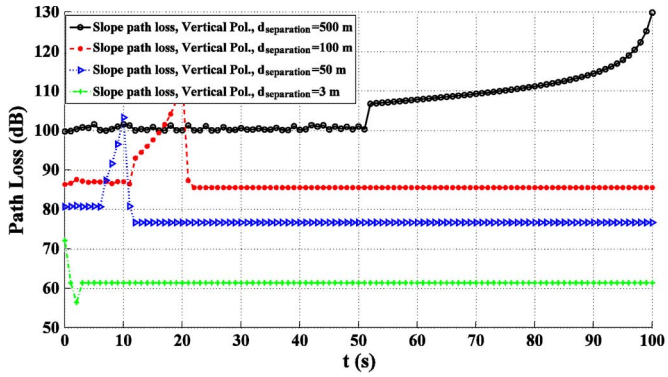

Fig. 6. Slope path loss versus time when $V1$ and $V2$ move at 5 m/s at separation distance values $d_{\text{separation}} = 3$ m, 50 m, 100 m, and 500 m, with slope height $H = 3$ m and tilt angle $\alpha = \pi/10$.

Fig. 6 shows the variation of path loss versus time. For the blue dotted line (triangles), $V1$ (back) and $V2$ (front) are 50 m away from each other at first, then $V2$ moves onto the slope, while for a time, $V1$ is still moving along the flat terrain (prior to the slope's bottom point), which corresponds to scenario 3 and where 3 rays (LOS, slope reflection, and flat ground reflection) exist. The path loss stays approximately constant at 81 dB. When $V2$ moves onto the slope top after about 2 s, the conditions quickly change to scenario 1, and this lasts for approximately 5 s. The path loss fluctuates by a very small amount around 81 dB. Since the LOS component is blocked by the slope crest at 6 s, the path loss rapidly increases to 100 dB. At approximately $t = 11$ s, $V1$ begins moving onto the slope, a LOS path reoccurs, which reduces the path loss rapidly to 80 dB. Then, $V1$ also arrives at the slope crest at 11 s, and the scenario changes from scenario 2 to the usual flat 2-ray. Thus, the path loss decreases to 78 dB and remains at that value for the remainder of the simulation. The conditions pertaining to the black solid line (circles) and red dashed lines (asterisks) are similar to those of the blue dotted line (triangles) except that only scenarios 1 and 3 exist for the black solid line (circles). For results of the green line (dash-dotted, "plus" symbols), the separation distance is our smallest value $d_{\text{separation}} = 3$ m. Here, at $t = 0$ s, both vehicles are on the flat terrain prior to the slope, and the conventional 2-ray model loss is 72 dB. At $t = 1$ s, both $V1$ and $V2$ are moving on the slope, and this is scenario 4. The path loss is 62 dB. For the following 1 s, $V2$ begins to move past the slope crest, whereas $V1$ continues to move on the slope, changing the scenario from 4 and 2. The path loss decreases to 58 dB. The two vehicles both move beyond the slope crest after 3 s, and the (2-ray) path loss becomes 62 dB and stays constant.

In practice of course, such abrupt attenuations, as shown in Fig. 6, will not occur, and actual path loss will follow a smoother curve. Additional multipath components from other objects in the environment (e.g., parked cars and buildings) may also be present and, along with diffuse-scattered components, will tend to make the path loss plots appear "noisy."

III. Measurement Results

To assess the accuracy of our slope path loss model for scenario 1, measurement data were collected at a slope near the campus of the University of South Carolina, Columbia, SC, via channel sounding equipment, on December 29, 2012. In the measurements, the slope is located at geographic coordinates North latitude 33.9888°, West longitude 81.02246°, and the slope was 3.49 m high with a 20.9° tilt. The measurements were on a section of Bull Street, between Heyward

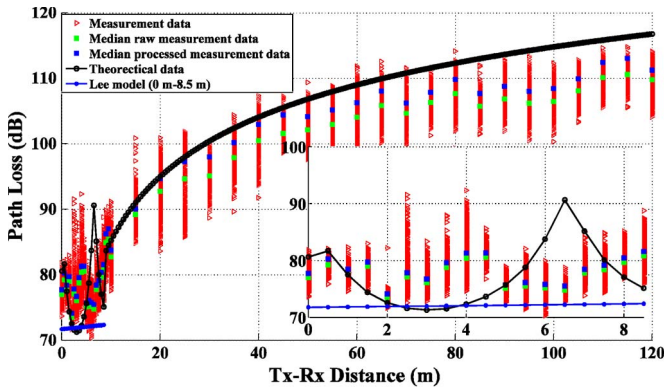

Fig. 7. Theoretical and measured path loss in a slope (scenario 1). Inset: detail for short distance; $d = 0 - 8.5$ m.

Street (slope bottom) and Whaley Street (slope top) in downtown Columbia.

Our measurement equipment is a modified version of the "Raptor" spread-spectrum-stepped correlator by Berkeley Varitronics System, Inc. [16]. The signal center frequency was 5.12 GHz. This spread-spectrum sounder used a chip rate of 50 MHz, which corresponds to a time-domain resolution of 20 ns. Vertical-oriented omnidirectional quarter-wave monopole antennas were used for both the Tx and the Rx. The transmit power was approximately 33 dBm. The output of the Rx came in the form of power-delay profiles (PDPs); hence, we summed up the power in all received components to obtain the total received power. The Tx and Rx antennas were each mounted on 0.9-m-high carts. The Tx was fixed at the bottom of the slope, and the Rx moved in steps of size 50 cm for the first 10 m and in steps of size 5 m for the remaining 110 m to the top of the slope.

Fig. 7 shows measured path loss versus Rx-slope crest distance, along with our analytical results. There are some buildings around this slope set back from the street on both sides of this slope. These buildings potentially provide additional paths via reflections to the Rx, which makes the measured path loss smaller than the theoretical value. To remove the effect of these extra multipath components to better compare with our analysis, we removed the longer-delayed multipath components after the peak (LOS) component and likely ground reflection and diffraction. The unprocessed measurement data and processed measurement data are denoted raw measurement data and modified measurement data, respectively. The median modified measurement data (blue squares) show an increase in path loss of approximately 2.5 dB compared with the median raw measurement data (green squares) in Fig. 7, bringing the measurement results within a few decibels of the analytical results.

At each distance, over 1000 PDPs were collected. Within the first 8.5 m, there is a reflected path along with the LOS path at the Rx; therefore, the path loss should follow the slope 2-ray model. In Fig. 7, we can see that the measurement data are distributed around the theoretical line, which supports our proposed slope 2-ray model. After the 8.5-m distance, the measured path loss increases because the LOS path is obstructed by the slope crest, which corresponds to the slope diffraction model. The Lee model is also used to compare with the measurement data. As shown in Fig. 7, the path loss of the Lee model is almost 8 dB smaller than that of the measurements and is not as accurate as our proposed model.

IV. Conclusion

In this paper, we have proposed path loss models for communication with low-height antennas on a slope, which can be separated into four scenarios. For scenarios that have not been addressed in the literature (scenarios 1 and 2) we derived mathematical expressions for the path loss at short distances and determined the critical condition for when to apply a slope diffraction model (computed using the knife-edge model) when the Tx and the Rx are at larger distances. Finally, we conducted measurements for scenario 1 on an actual slope to compare results with those of our proposed path loss model. The measured data agree fairly well with that computed by our theoretical model, supporting our model's utility.

References

[1] Y. Okumura, E. Ohmori, T. Kawano, and K. Fukuda, "Field strength and its variability in VHF and UHF land mobile radio service," *Rev. Elect. Commun. Lab.*, vol. 16, no. 9/10, pp. 825–873, Sep. 1968.

[2] R. Edwards and J. Durkin, "Computer prediction of service area for VHF mobile radio networks," *Proc. Inst. Elect. Eng.*, vol. 116, no. 9, pp. 1493–1500, Sep. 1969.

[3] C. E. Dadson, "Radio network and radio link surveys derived by computer from a terrain data base," presented at the NATO-AGARD Conference, Lisbon, Portugal, Dec. 1979, Paper CPP-269.

[4] A. G. Longley and P. L. Rice, "Prediction of tropospheric radio transmission over irregular terrain: A computer-based method," Environ. Sci. Services Admin., Boulder, CO, USA, ESSA Tech. Rep. ERL 79-ITS67, 1968.

[5] B. Thelot, "Method of calculating the propagation parameters used in the VHF and UHF bands," *EUB Rev.*, pp. 76–81, 1981.

[6] D. S. Paunovic, D. C. Stojanovic, and I. S. Stojanovic, "Choice of a suitable method for the prediction of field strength in planning land mobile radio systems," *IEEE Trans. Veh. Technol.*, vol. VT-33, no. 3, pp. 259–265, Aug. 1984.

[7] J. P. Murphy, "Statistical propagation model for irregular terrain model paths between transportable and mobile antennas," in *Proc. NATO-AGARD Conf.*, 1970, pp. 49.1–49.20.

[8] W. C. Y. Lee, *Mobile Communication Engineering*. New York, NY, USA: McGraw-Hill, 1982.

[9] T. Ohira, T. Hirai, S. Tomisato, and M. Hata, "A study of mobile path loss estimation models for a sloping terrain area in cellular systems," in *Proc. 18th Asia-Pac. Conf. Commun.*, Jeju, Korea, Oct. 15–17, 2012, pp. 472–477.

[10] M. Nisirat, M. Ismail, L. Nissirat, and S. Al Khawaldeh, "Micro cell path loss estimation by means of terrain slope for 900 and 1800 MHz," in *Proc. Int. Conf. Comput. Commun. Eng.*, Kuala Lumpur, Malaysia, Jul. 3–5, 2012, pp. 670–674.

[11] C.-X. Wang, X. Cheng, and D. Laurenson, "Vehicle-to-vehicle channel modeling and measurements: Recent advances and future challenges," *IEEE Commun. Mag.*, vol. 47, no. 11, pp. 96–103, Nov. 2009.

[12] L. Cheng, B. E. Henty, D. D. Stancil, F. Bai, and P. Mudalige, "Mobile vehicle-to-vehicle narrow-band channel measurement and characterization of the 5.9 GHz frequency band," *IEEE J. Sel. Areas Commun.*, vol. 25, no. 8, pp. 1501–1516, Oct. 2007.

[13] J. Karedal, N. Czink, A. Paier, F. Tufvesson, and A. F. Molisch, "Path loss modeling for vehicle-to-vehicle communications," *IEEE Trans. Veh. Technol.*, vol. 60, no. 1, pp. 323–328, Jan. 2011.

[14] X. Cheng, C.-X. Wang, D. Laurenson, S. Salous, and A. Vasilakos, "An adaptive geometry-based stochastic model for non-isotropic MIMO mobile-to-mobile channels," *IEEE Trans. Wireless Commun.*, vol. 8, no. 9, pp. 4824–4835, Sep. 2009.

[15] J. D. Parsons, *The Mobile Radio Propagation Channel*. New York, NY, USA: Wiley, 2000.

[16] Berkeley Varitronics, Inc., Metuchen, NJ, USA, Dec. 12, 2012. [Online]. Available: http://www.bvsystems.com